

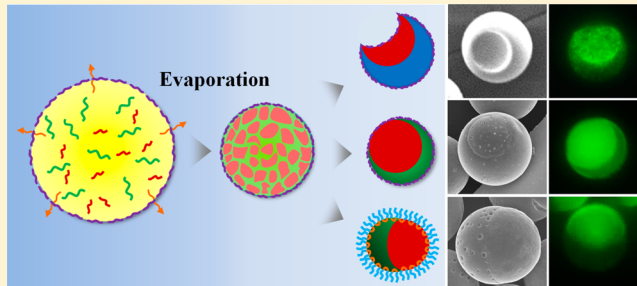
## Anisotropic Microparticles Created by Phase Separation of Polymer Blends Confined in Monodisperse Emulsion Drops

Nam Gi Min, Bomi Kim, Tae Yong Lee, Dahn Kim, Doh C. Lee, and Shin-Hyun Kim\*

Department of Chemical and Biomolecular Engineering (BK21 Plus Program) and KINC, KAIST, 291 Daehak-ro, Yuseong-gu, Daejeon, 305-701 Korea

### Supporting Information

**ABSTRACT:** Anisotropic microparticles are promising as a new class of colloidal or granular materials due to their advanced functionalities which are difficult to achieve with isotropic particles. However, synthesis of the anisotropic microparticles with a highly controlled size and shape still remains challenging despite their intense demands. Here, we report a microfluidic approach to create uniform anisotropic microparticles using phase separation of polymer blends confined in emulsion drops. Two different polymers are homogeneously dissolved in organic solvent at low concentration, which is microfluidically emulsified to produce oil-in-water emulsion drops. As the organic solvent diffuses out, small domains are formed in the emulsion drops, which are then merged, forming only two distinct domains. After the drops are fully consolidated, uniform anisotropic microparticles with two compartments are created. The shape of the resulting microparticles is determined by combination of a pair of polymers and type of surfactant. Spherical microparticles with eccentric core and incomplete shell are prepared by consolidation of polystyrene (PS) and poly(lactic acid) (PLA), and microparticles with single crater are formed by consolidation of PS and poly(methyl methacrylate) (PMMA); both emulsions are stabilized with poly(vinyl alcohol) (PVA). With surfactants of triblock copolymer, acorn-shaped Janus microparticles are obtained by consolidating emulsion drops containing PS and PLA. This microfluidic production of anisotropic particles can be further extended to any combination of polymers and colloids to provide a variety of structural and chemical anisotropy.



### INTRODUCTION

Isotropic microparticles have been synthesized by emulsion or dispersion polymerization with a high controllability over their size and property and utilized in various fields including chemicals, cosmetics, pharmaceuticals, and electronics industries.<sup>1</sup> For example, monodisperse microparticles are used as spacers to maintain film thickness of liquid crystals in display panels.<sup>2</sup> As a new class of colloidal materials, anisotropic microparticles are promising due to their advanced functionality for high-end applications.<sup>3</sup> For example, Janus microspheres can be used as active pigments for display,<sup>4,5</sup> and amphiphilic microparticles can serve as colloidal surfactants for long-term stabilization and immobilization of fluid–fluid interfaces.<sup>6,7</sup> Dimpled microparticles are recently employed as colloidal building blocks to study colloidal interaction and construct unconventional colloidal assemblies.<sup>8</sup> Nevertheless, synthesis of anisotropic microparticles is still challenging. Although post-processing of isotropic microparticles has enabled the production of dumbbell-shaped, ellipsoidal, and oblate microparticles,<sup>9–11</sup> only few sets of materials are available.

Emulsion drops provide a spherical confining geometry for polymers and colloids, thereby enabling the creation of microparticles through their consolidation.<sup>12,13</sup> Moreover, drops containing two or more distinct components can produce

anisotropic or nanostructured microparticles. For example, two immiscible polymers dissolved in a single drop can produce microparticles with various configurations through phase separation depending on interfacial energies,<sup>14,15</sup> and block copolymers can exhibit microphase separation in the drop, thereby creating regular nanostructure in each microparticle.<sup>16</sup> However, emulsion drops prepared by bulk emulsification yield polydisperse microparticles, thereby restricting their applications. To overcome such a limitation, drop-based microfluidics have been employed to produce uniform emulsion drops, albeit only on a drop-by-drop basis.<sup>17</sup> Phase separation of polymer–polymer or polymer–surfactant in uniform drops leads to the formation of monodisperse Janus or dumbbell-shaped microparticles.<sup>18,19</sup> However, production and design of monodisperse anisotropic microparticles are still in the early stage, and there remains intense demand for new class of microparticles with structural and compositional anisotropy.

In this paper, we report a facile microfluidic strategy to create monodisperse anisotropic microparticles by phase separation of polymer blends confined in emulsion drops. With a glass

Received: November 10, 2014

Revised: December 28, 2014

Published: December 30, 2014

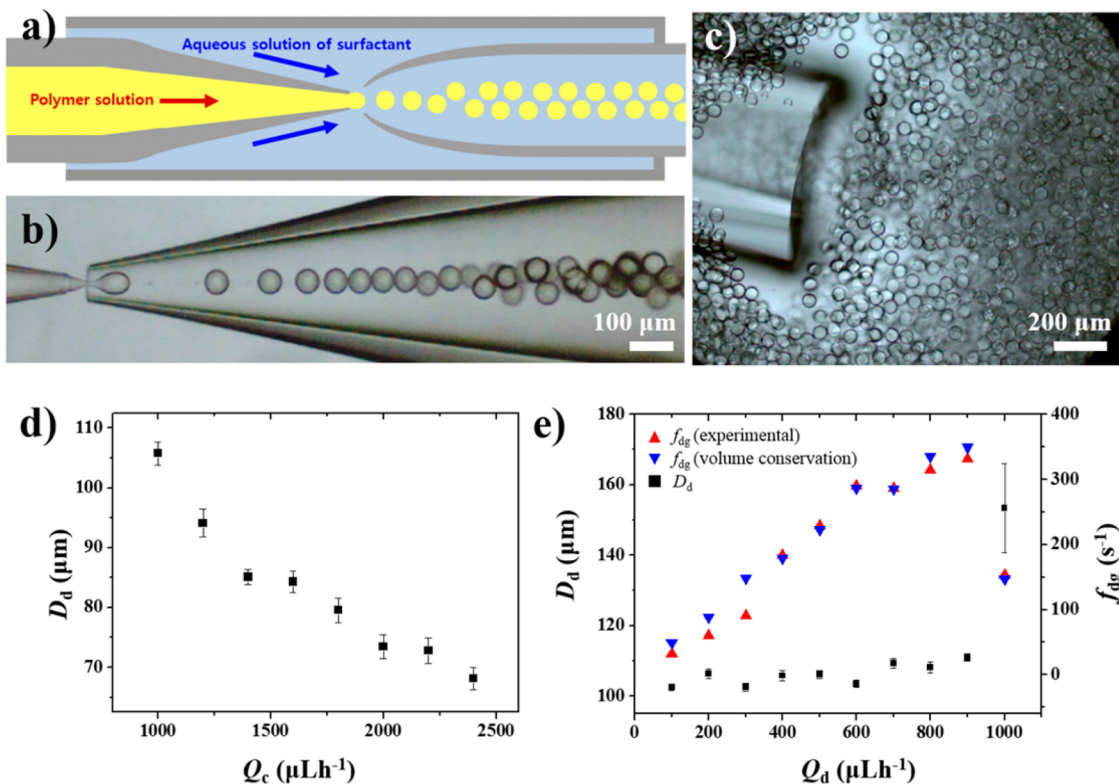


**Figure 1.** (a) Schematic illustration of a microfluidic device composed of the left injection and right collection capillaries for the production of oil-in-water emulsion droplets. (b, c) Optical microscope (OM) images showing the generation of monodisperse emulsion droplets at the tip of the injection capillary and the accumulation of the droplets from the exit of the collection capillary. (d, e) Influence of volumetric flow rates of dispersed,  $Q_d$ , and continuous,  $Q_c$ , phases on droplet diameter,  $D_d$ , where value of  $Q_d$  is maintained at  $400 \mu\text{L h}^{-1}$  in part d and the value of  $Q_c$  is maintained at  $1000 \mu\text{L h}^{-1}$  in part e. The error bars denote standard deviation of the droplet diameter. The generation frequency of droplets,  $f_{dg}$ , is included in right y-axis in part e, where red triangles denote  $f_{dg}$  measured from experiment and blue inverted triangles denote  $f_{dg}$  calculated from volume conservation.

microfluidic device, oil-in-water (O/W) emulsion droplets are prepared in a highly controlled fashion, which serve as a confining geometry of two immiscible polymers. The polymers exhibit phase separation as organic solvent diffuses out from the oil droplets, which then evolve to anisotropic microparticles as the droplets are fully consolidated. Interestingly, microparticles with a large single crater can be prepared from spherical emulsion droplets; this involves indentation of the interface in the final stage of consolidation due to early hardening of incomplete open shell. In addition, either spherical core–shell or acorn-shaped Janus microparticles can be selectively created by employing different sets of interfacial stabilizers and pairs of two immiscible polymers. This production scheme can be further utilized for unlimited sets of polymeric or colloidal materials owing to high chemical resistance of glass capillary devices. Moreover, production throughput can be potentially enhanced through parallelization of the devices.<sup>20</sup>

## MATERIALS AND METHODS

**Materials.** Two of three different polymers, polystyrene (PS,  $M_w$  35 000, Sigma-Aldrich), poly(methyl methacrylate) (PMMA,  $M_w$  350 000, Sigma-Aldrich), and poly(lactic acid) (PLA,  $M_w$  20 000–30 000, Polyscience, Inc.), are dissolved in toluene (Sigma-Aldrich) to have concentration of 0.75 w/v% for each polymer; this organic solution is used as a dispersed phase of emulsions. To selectively label PS domain during consolidation, CdSe/ZnS quantum dot nanoparticles with diameter of 6 nm capped with oleic acid and trioctylphosphine are synthesized<sup>21</sup> and additionally dispersed in the organic solution. As a continuous phase, either 10 w/w% aqueous solution of poly(vinyl alcohol) (PVA,  $M_w$  13 000–23 000, Sigma-Aldrich) or aqueous mixture

of 1.5 w/w% triblock copolymer of poly(ethylene glycol)-poly(propylene glycol)-poly(ethylene glycol) (PEO–PPO–PEO, F108,  $M_n$  14 600, Sigma-Aldrich) and 8.5 w/w% poly(ethylene glycol) (PEG,  $M_n$  6000, Sigma-Aldrich) is used; PEG is added to increase viscosity of the continuous phase.

**Device Preparation and Characterization.** Two cylindrical capillaries (1B100F-6, World Precision Instruments, Inc.) are tapered by micropipette puller (P97, Sutter Instrument), one of which is then sanded to have larger orifice diameter. These two capillaries are coaxially assembled in a square capillary (OD 1.5 mm, ID 1.05 mm, Harvard borosilicate square tubing) without chemical modification. Volumetric flow rates are controlled by syringe pumps (Legato 100, KD Scientific). The production of emulsion drops is observed with inverted optical microscope (Eclipse TS100, Nikon) equipped with a high speed camera (Phantom Miro eX2, Vision Research). The drops are collected in a glass dish at room temperature for 2 h. For analysis of resultant microparticles, fluorescence microscope (Eclipse Ti, Nikon) and scanning electron microscope (SEM, S-4800, Hitachi) are used.

## RESULTS AND DISCUSSION

**Preparation of Monodisperse Emulsion Droplets.** To produce uniform microparticles, monodisperse O/W emulsion droplets are prepared as a template using a glass capillary microfluidic device. The device is composed of two facing tapered cylindrical capillaries with different orifice diameters of 40 and 80  $\mu\text{m}$  which are nested in a square capillary. The dispersed phase is injected through the cylindrical capillary with smaller orifice, and the continuous phase is injected through the interstices between the cylindrical and square capillaries, where the other interstices are closed as shown in Figure 1a. The cylindrical capillary with larger orifice is used for collection of

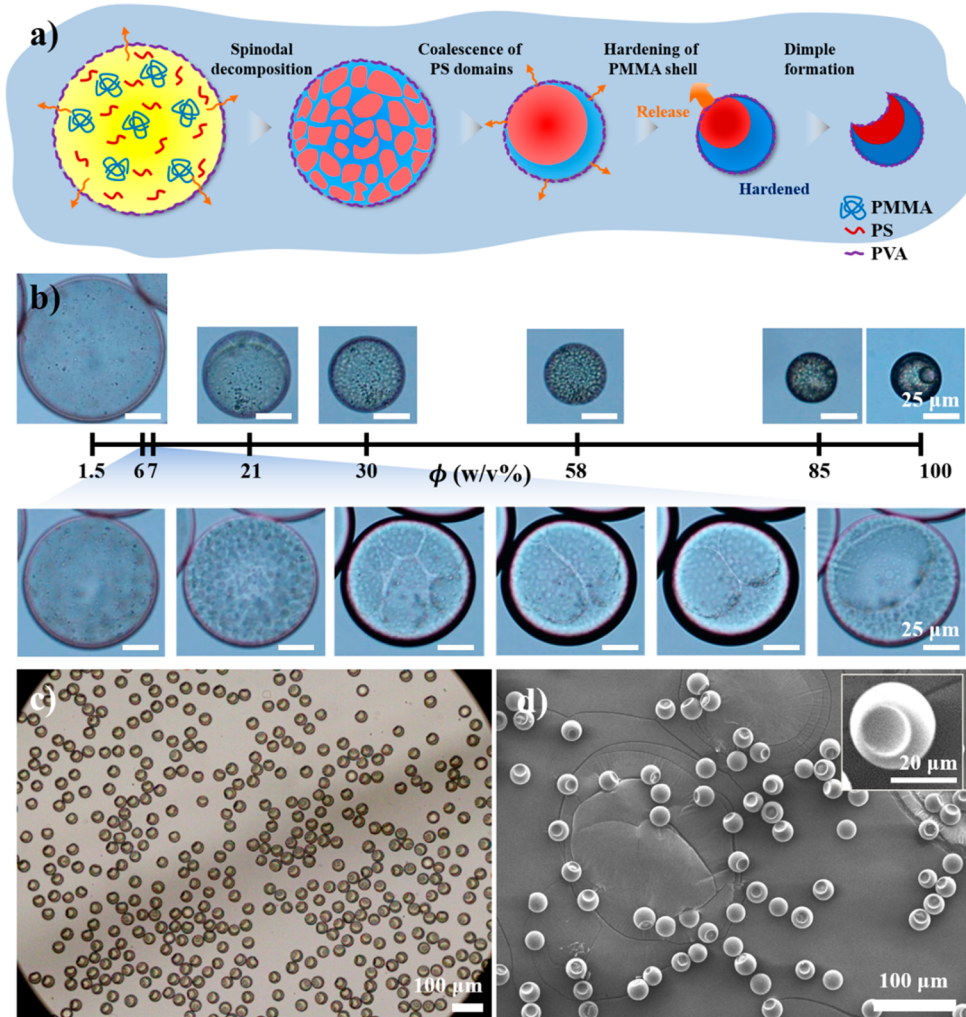


**Figure 2.** (a, b) Series of cartoons and OM images showing the formation of dimpled microparticle by consolidation of toluene emulsion drop containing polystyrene (PS) and poly(methyl methacrylate) (PMMA) dispersed in aqueous solution of poly(vinyl alcohol) (PVA). Evolution of internal structure is shown in part b, where scales are set to be the same for direct size comparison. (c, d) OM and scanning electron microscope (SEM) images of highly monodisperse dimpled microparticles.

emulsion droplets, where the small opening of the capillary helps increase linear flow velocity of the continuous phase, thereby exerting high drag force on the drop hanging on the tip of the injection capillary. Highly monodisperse emulsion droplets are generated at the tip of the injection capillary in a dripping mode. For example, we prepare monodisperse toluene droplets, containing PS and PMMA, dispersed in the aqueous solution of PVA in a dripping mode, as shown in Figure 1b. The droplets flow through the collection capillary, and are then accumulated in a glass dish, as shown in Figure 1c. The droplets are stable against coalescence due to stabilization of the interface with surfactants of PVA, thereby producing monodisperse microparticles after organic solvent is fully depleted.

At every moment of breakup in a dripping mode, the drag force exerted by continuous phase is balanced with the capillary force by the tip, thereby providing all the same volume of droplets; the drag force increases as the drop hanging on the tip grows, while the capillary force remains almost constant.<sup>22</sup> To operate the device in the dripping mode, we investigate the influence of flow rates on the breakup behavior as shown in Figure S1 of the Supporting Information. Monodisperse droplets are generated in a dripping mode for a relatively low flow rate of the dispersed

phase, while polydisperse and large drops are generated in a broadening jetting mode for the flow rate larger than certain value. Operating in the dripping mode, droplet size and generation frequency can be controlled by adjusting flow rates of the continuous and dispersed phases. As the flow rate of continuous phase,  $Q_c$ , is increased from 1000 to 2400  $\mu\text{L h}^{-1}$ , while maintaining constant flow rate of dispersed phase,  $Q_d$ , of 400  $\mu\text{L h}^{-1}$ , droplet diameter,  $D_d$ , is monotonically decreased from 105 to 68  $\mu\text{m}$ , as shown in Figure 1d and Movie S1 of the Supporting Information; coefficient of variation (CV) of  $D_d$  remains smaller than 3% for all flow rates. This is caused by increase of drag force on the hanging droplets as  $Q_c$  increases. For a wide range of  $Q_d$  from 100 to 900  $\mu\text{L h}^{-1}$ ,  $D_d$  remains almost unchanged as shown in Figure 1e, where  $Q_c$  is maintained at constant value of 1000  $\mu\text{L h}^{-1}$ ; deviation of  $D_d$  from the average in the range of  $Q_d$  is less than 5%. This is because  $Q_d$  insignificantly influences both the drag force and capillary force. Instead,  $Q_d$  determines the frequency of droplet generation,  $f_{dg}$ , as estimated from volume conservation of dispersed phase,  $f_{dg} = 6Q_d(\pi D_d^3)^{-1}$ . Because  $D_d$  is almost constant,  $f_{dg}$  is linearly proportional to  $Q_d$  in dripping mode as shown in Figure 1e, where values of  $f_{dg}$  are obtained by analysis of

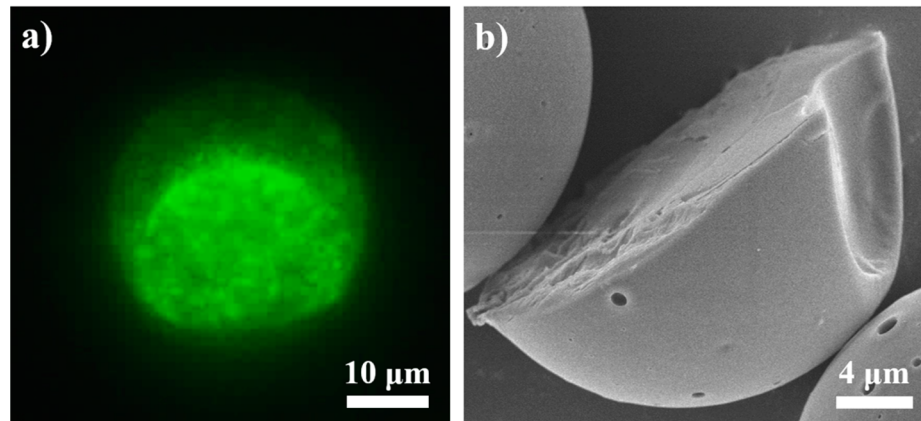


**Figure 3.** (a) Fluorescence microscope image of dimpled microparticle prepared from toluene drop containing PS, PMMA, and CdSe/ZnS quantum dot (QD) nanoparticles. The QD particles are preferentially segregated in the eccentric core of dimpled microparticle. (b) SEM image showing cross-section of dimpled microparticle.

movies taken by a high frames per second of 21 052; the values are in good accord with  $f_{dg}$  calculated from the volume conservation. This proportionality can be roughly confirmed by Supporting Information Figure S2 and Movie S2. At maximum  $Q_d$  for a dripping mode,  $900 \mu\text{L h}^{-1}$ ,  $f_{dg}$  is 331 Hz and CV of  $D_d$  still remains as small as 1%. The increase of the frequency while maintaining size uniformity is important for enhancement of production throughput of microparticles. For further increase of  $Q_d$  to  $1000 \mu\text{L h}^{-1}$ , transition from dripping to jetting occurs, resulting in polydisperse large droplets as shown in Figure 1e; CV of  $D_d$  becomes 8%.

**Dimpled Microparticles.** As organic solvent diffuses out from emulsion droplets to continuous phase during incubation, droplets become shrunken, and a binary mixture of polymers dissolved in the droplets is concentrated, leading to the phase separation. The solvent is finally depleted, which results in the formation of microparticles composed of two distinct compartments. The pair of two different polymers and type of surfactant influence the structure and shape of the solid microparticles.

The emulsion droplets of toluene containing PS and PMMA dispersed in aqueous solution of PVA transform to dimpled microparticles during the droplet shrinkage, as schematically illustrated in Figure 2a. It is interesting that nonspherical particles with a concave surface are formed from spherical emulsion droplets. To elucidate the formation of such an unconventional structure, we monitor a single droplet in a course of consolidation, as shown in Figure 2b; large emulsion droplet with  $D_d = 116 \mu\text{m}$  is used to clearly observe the evolution. In the beginning, the droplet has a low concentration of polymers as 1.5 w/v%; each polymer has concentration of 0.75 w/v%. Because polymer mass is conserved in the droplet during the shrinkage, the concentration,  $\phi$ , can be estimated from diameter of the shrinking droplets,  $D_s$ , as  $\phi_0(D_d/D_s)^3$ . A drastic change is observed at  $\phi = 6\text{--}7 \text{ w/v\%}$  as shown in a series of optical microscope images in the bottom row of Figure 2b. The homogeneous droplet becomes heterogeneous as PS-rich and PMMA-rich phases are formed and separated. In the beginning of the phase separation, very small domains of each phase are generated over the entire volume of droplet (this is referred to as spinodal decomposition), which are then merged with their neighbors, finally forming a single domain; this dynamic internal transformation is clearly shown in Movie S3 of the Supporting Information. As the droplet is further shrunken, two domains of eccentric core of PS-rich phase and shell of PMMA-rich phase are

formed at which the core is partially exposed to the surrounding, as shown in the second image of top row. This configuration is formed by minimum total interfacial energy contributed from three interfaces of PS-rich phase/continuous phase, PMMA-rich phase/continuous phase, and PS-rich phase/PMMA-rich phase; spreading parameter,  $S$ , which is defined as  $\gamma_{\text{PS-C}} - (\gamma_{\text{PMMA-C}} + \gamma_{\text{PS-PMMA}})$  is weakly negative, forming partially exposed core and incomplete shell,<sup>7,23</sup> where  $\gamma_{\text{PS-C}}$ ,  $\gamma_{\text{PMMA-C}}$ , and  $\gamma_{\text{PS-PMMA}}$  indicate interfacial energies of corresponding interfaces. The droplet continuously shrinks while maintaining spherical shape before  $\phi = 85 \text{ w/v\%}$ ; the droplet aligns to have PS-rich domain upward at  $\phi = 30$  and 58 w/v%, which makes it difficult to distinguish two distinct domains. At the last stage of consolidation from  $\phi = 85 \text{ w/v\%}$  to 100 w/v%, a single dimple forms and grows as shown in the last two images. We attribute the dimple formation to hardening of PMMA shell ahead of that of eccentric PS core.<sup>15</sup> In the last stage, a small volume of toluene remains, which prefers to stay in PS domain due to its higher affinity with PS than PMMA; polymer–solvent interaction parameter between toluene and PS is 0.25 for polymer volume fraction of 0.8 at 23.5 °C and that between toluene and PMMA at the same condition is 0.45.<sup>24</sup> This can lead to earlier hardening of PMMA shell and subsequent indentation at the surface of relatively viscoelastic PS-rich domain for final removal of all the residual toluene. The scenario of phase separation and dimple formation is illustrated in Figure 2a. The complete consolidation of the emulsion drops with  $D_d = 116 \mu\text{m}$  and  $\phi_0 = 1.5 \text{ w/v\%}$  takes 50 min at room temperature; the consolidation is faster for smaller drops with higher concentration of polymers.

Uniform microparticles with a single dimple can be prepared from monodisperse emulsion droplets, as shown in Figure 2c,d; a lower magnification image is included in Supporting Information Figure S3 to show reliability of this microfluidic method. The droplets with diameter of  $96 \mu\text{m}$  containing 0.75 w/v% PMMA and 0.75 w/v% PS are consolidated to microparticles with diameter of  $26 \mu\text{m}$ ; this is roughly consistent with mass balance of  $D_d(\phi_0/\phi_f)^{1/3}$ , where  $\phi_f$  is final concentration of polymers and set to be 100 w/v%. The dimples on microparticles are also uniform; they have average size of  $14.8 \mu\text{m}$  and CV of 2.6%. Two distinct domains of PS and PMMA can be clearly observed with optical microscope due to their refractive index contrast as shown in Figure 2c; refractive indexes of PS and PMMA are 1.59 and 1.49, respectively. Shape and size of dimples are also clearly observed with SEM as shown in Figure 2d.

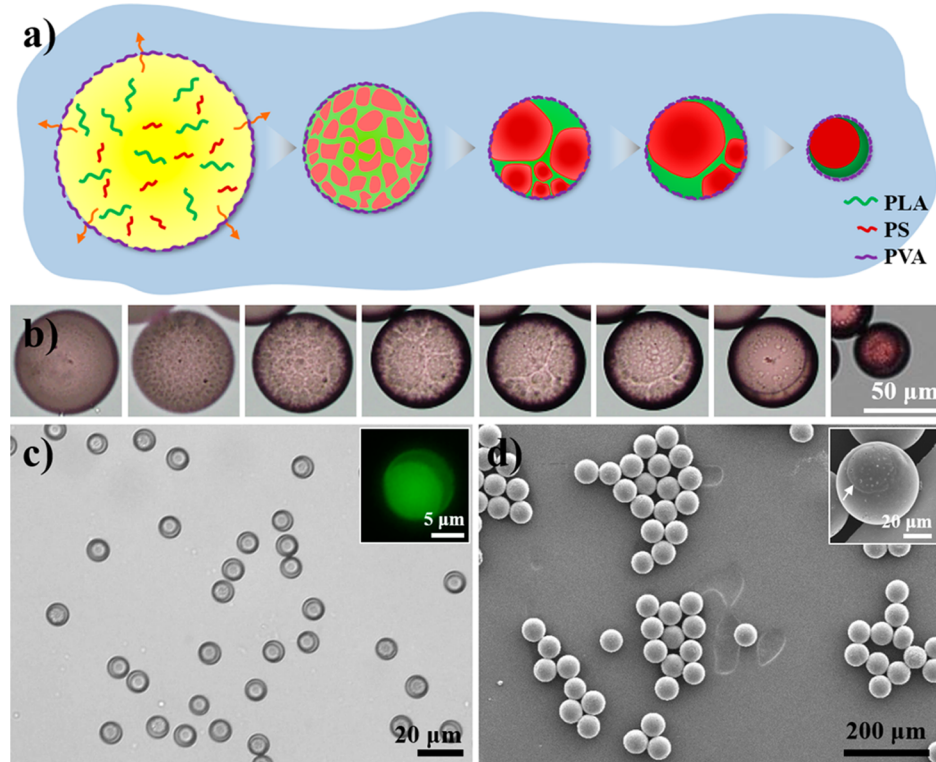


**Figure 4.** (a, b) Series of cartoons and OM images showing the formation of spherical microparticle with eccentric core and incomplete shell by consolidation of emulsion drop containing PS and poly(lactic acid) (PLA) dispersed in aqueous solution of PVA. (c) OM image of monodisperse core–shell microparticles. Inset shows fluorescence microscope image of core–shell microparticles of which eccentric PS-rich core is preferentially stained with QD nanoparticles. (d) SEM image of core–shell microparticles. A boundary between two domains is indicated with an arrow in the inset.

To confirm the composition of core and shell and further prove the scenario, CdSe/ZnS quantum dot nanoparticles with diameter of 6 nm are additionally included in the toluene drops containing PS and PMMA; nanoparticles are capped with oleic acid and trioctylphosphine. It turns out that the quantum dot nanoparticles are preferentially segregated in PS domains during consolidation. This is contradictory to a previous study which reported that oleic acid renders the surface of the nanoparticles to prefer PMMA.<sup>25</sup> We attribute this to trioctylphosphine which might have higher affinity to PS than PMMA and lead to the preferential segregation in PS domain. The consolidated microparticle exhibits strong fluorescence from the eccentric core and weak signal from the shell as shown in Figure 3a. This indicates that the core is PS-rich and the shell is PMMA-rich, as we expect in Figure 2a; more hydrophobic PS-rich domain is wrapped with less hydrophobic PMMA domain. We model this geometry with Surface Evolver to estimate  $\gamma_{\text{PMMA-C}}$  and  $\gamma_{\text{PS-C}}$  relative to  $\gamma_{\text{PS-PMMA}}$  as shown in Supporting Information Figure S4;<sup>26</sup>  $\gamma_{\text{PMMA-C}}/\gamma_{\text{PS-PMMA}} = 3.5838$  and  $\gamma_{\text{PS-C}}/\gamma_{\text{PS-PMMA}} = 4.4913$ , which gives weakly negative spreading parameter of  $-0.0922 \times \gamma_{\text{PS-PMMA}}$ . Although the dimple formation is reminiscent of shell buckling,<sup>27</sup> our scenario does not include the buckling of solid shell, but does involve consolidation of PS polymer in the hardened PMMA bowl; if the dimple were formed by crumbling of hardened shell, there would be internal cavity. To confirm the absence of cavity, we cut microparticle with a razor blade and observe internal structure with SEM as shown in Figure 3b. The microparticle is dense and does not possess any internal cavity, proving that the dimple is not formed by the buckling of shell.

**Spherical Core–Shell Microparticles.** The formation of dimple in the microparticles composed of PS and PMMA is

attributed to earlier hardening of PMMA shell. To avoid this and make spherical core–shell microparticles, we replace PMMA with PLA, while maintaining all other conditions; interaction parameter between toluene and PLA is expected to be smaller than that between toluene and PMMA. The small domains of PS-rich and PLA-rich phases are generated on the onset of phase separation, which are then merged into large ones as the polymers are concentrated, as shown in Figure 4a,b. As the concentration is further increased, eccentric core of PS-rich phase and incomplete shell of PLA-rich phase are formed due to weakly negative spreading parameter in the same manner as the pair of PS and PMMA. This phase separation is also shown in Supporting Information Movie S4. However, the emulsion drops finally evolve to spherical core–shell microparticles without dimple formation, unlike the pair of PS and PMMA, as shown in the last image of Figure 4b. This indicates that there is no early hardening of incomplete PLA shell. High uniformity of the spherical core–shell microparticles can be achieved by employing monodisperse emulsion drops as shown in Figure 4c, where the microparticles with average diameter of 9 μm are prepared from emulsion drops with average diameter of 33 μm. When the CdSe/ZnS quantum dot nanoparticles are included in the emulsion drops, they are preferentially segregated in the eccentric core as shown in the inset of Figure 4c, proving that the core is PS-rich and shell is PLA-rich; this geometry is modeled with Surface Evolver as shown in Supporting Information Figure S5, which provides  $\gamma_{\text{PLA-C}}/\gamma_{\text{PS-PLA}} = 2.3855$  and  $\gamma_{\text{PS-C}}/\gamma_{\text{PS-PLA}} = 3.3546$ , and therefore weakly negative spreading parameter of  $-0.0309 \times \gamma_{\text{PS-PLA}}$ . The uniform size of the microparticles and the partial exposure of the eccentric core

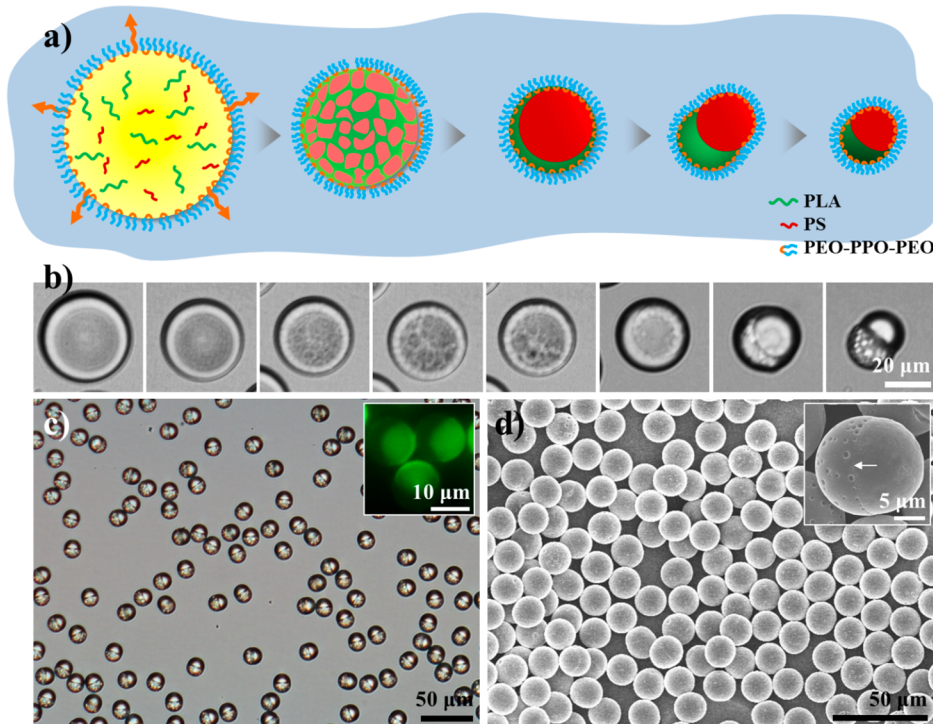


**Figure 5.** (a, b) Series of cartoons and OM images showing the formation of acorn-shaped Janus microparticle by consolidation of toluene emulsion drop containing PS and PLA dispersed in aqueous solution of triblock copolymers of poly(ethylene oxide)-poly(propylene oxide)-poly(ethylene oxide) (PEO-PPO-PEO). (c) OM image of monodisperse Janus microparticles. Inset is fluorescence microscope image of acorn-shaped microparticles of which PS-rich domain is preferentially stained with QD nanoparticles. (d) SEM image of Janus microparticles. A boundary between two domains is indicated with an arrow in the inset.

to the surrounding are further confirmed by SEM images in Figure 4d and its inset.

**Acorn-Shaped Janus Microparticles.** The configuration of microparticles is significantly influenced by interfacial energies. Surfactant molecules dissolved in the continuous phase adsorb at the interfaces of emulsion droplet and alter the interfacial energies, thereby possibly changing the configuration of consolidated microparticles. When the surfactant molecule of PVA is replaced with PEO-PPO-PEO triblock copolymer, while maintaining the same composition of the dispersed phase, PS and PLA dissolved in toluene, the configuration of microparticles is dramatically changed from eccentric core and incomplete shell structure to acorn-shaped Janus structure, as shown in Figure 5. Although small domains are generated and then merged to form eccentric core and incomplete shell in the early and middle stages of phase separation in the similar manner to drop stabilized with PVA, the drop further evolves to acorn-shaped structure as shown in Figure 5b; this phase separation is also shown in Movie S5 of the Supporting Information. Unlike the spherical core–shell structure prepared from drops stabilized by PVA, there is a concave outer interface along the boundary between two domains in the acorn-shaped drop, as shown in the last image of Figure 5b; at this moment, the drop is not fully consolidated yet. This geometry can be formed by dewetting of PLA-rich phase. Although PS-rich domain is relatively hydrophobic in comparison with PLA, which usually leads to the formation of core–shell structure, interfacial energy between PS-rich domain and continuous phase can be significantly reduced by the surfactant of PEO-PPO-PEO triblock copolymers, leading to considerably negative value of spreading parameter and resulting in the dewetting to form the acorn-shaped structure.<sup>23</sup> The emulsion drops are finally consolidated to solid microparticles,

while maintaining the overall Janus configuration as shown in Figure 5c. During this final consolidation, the curvature of the outer surface at the boundary between two domains is reduced, as shown in Figure 5d and its inset; this also entails the reduction of aspect ratio of the Janus particles. The quantum dot nanoparticles included in the drops are preferentially segregated in PS-rich domain of the consolidated microparticles, which shows the shape of inner boundary between two domains as shown in the inset of Figure 5c; the PS-rich domain has a convex boundary, whereas the PLA-rich domain has a concave one. We model this geometry with Surface Evolver as shown in Supporting Information Figure S6, which provides  $\gamma_{\text{PLA-C}}/\gamma_{\text{PS-PLA}} = 2.3800$  and  $\gamma_{\text{PS-C}}/\gamma_{\text{PS-PLA}} = 3.2573$ , and therefore negative spreading parameter of  $-0.1227 \times \gamma_{\text{PS-PLA}}$ ; this value is 4-fold larger than that of the PVA-stabilized one.

## CONCLUSION

We have demonstrated a microfluidic approach to create uniform anisotropic microparticles using phase separation of polymer blends confined in emulsion droplets. Highly monodisperse O/W emulsion droplets are prepared in a capillary microfluidic device, which serves as a template to concentrate polymer blends and induce their phase separation. Depending on sets of materials, a pair of polymers and surfactant, one of three distinct structures (dimpled core–shell, spherical core–shell, and acorn-shaped Janus microparticles) is selectively created after complete consolidation. Of particular interest is that anisotropic geometries are prepared from isotropic emulsion drops. The phase separation of polymers in the emulsion drops leads to either eccentric core–shell or acorn-shaped geometries at equilibrium state depending on interfacial energy. The core–shell can be further kinetically evolved to dimpled geometry when the

incomplete shell is hardened earlier than the eccentric core. Our microfluidic approach can be extended to create anisotropic microparticles with unlimited sets of polymeric or colloidal materials. For example, two or more different color pigments can be involved into their own compartments of single microparticles using their preferential segregation in specific domain;<sup>28</sup> the microparticles can display distinct colors depending on their alignment. In addition, sets of biodegradable or environment-sensitive polymers can be confined in emulsion drops to encapsulate multiple ingredients, which are then released from microparticles in a highly controlled fashion due to different biodegradability and environment-response of each compartment.<sup>29,30</sup> Therefore, our microfluidic production of anisotropic microparticles will provide new opportunity for a wide range of applications including paint composites and drug or cosmetic carriers.

## ■ ASSOCIATED CONTENT

### Supporting Information

Flow behavior as a function of volumetric flow rates of dispersed and continuous phases. Optical microscope and SEM images showing monodisperse microparticles. Movies S1–5 show the generation of drops in microfluidic devices and phase separation in the shrinking emulsion drops. This material is available free of charge via the Internet at <http://pubs.acs.org>.

## ■ AUTHOR INFORMATION

### Corresponding Author

\*Phone: +82 42 350 3911. Fax: +82 42 350 3910. E-mail: kim.sh@kaist.ac.kr.

### Notes

The authors declare no competing financial interest.

## ■ ACKNOWLEDGMENTS

This work was supported by the KAIST HRHRP (Project No. N10130008) and the Midcareer Researcher Program (2014R1A2A2A01005813) through the National Research Foundation (NRF) grant funded by the Ministry of Science, ICT and Future Planning (MSIP).

## ■ REFERENCES

- (1) Arshady, R. Suspension, emulsion, and dispersion polymerization: A methodological survey. *Colloid Polym. Sci.* **1992**, *270*, 717–732.
- (2) Hamon, O. Process for positioning spacer beads in flat display screens. U.S. Patent 5,558,732, Dec 23, 1994.
- (3) Yang, S.-M.; Kim, S.-H.; Lim, J.-M.; Yi, G.-R. Synthesis and assembly of structured colloidal particles. *J. Mater. Chem.* **2008**, *18*, 2177–2190.
- (4) Nisisako, T.; Torii, T.; Takahashi, T.; Takizawa, Y. Synthesis of monodisperse bicolored Janus particles with electrical anisotropy using a microfluidic co-flow system. *Adv. Mater.* **2006**, *18*, 1152–1156.
- (5) Yu, Z.; Wang, C.-F.; Ling, L.; Chen, L.; Chen, S. Triphase microfluidic-directed self-assembly: Anisotropic colloidal photonic crystal supraparticles and multicolor patterns made easy. *Angew. Chem., Int. Ed.* **2012**, *51*, 2375–2378.
- (6) Kim, S.-H.; Lee, S. Y.; Yang, S.-M. Janus microspheres for a highly flexible and impregnable water-repelling interface. *Angew. Chem., Int. Ed.* **2010**, *49*, 2535–2538.
- (7) Kim, S.-H.; Abbaspourrad, A.; Weitz, D. A. Amphiphilic crescent-moon-shaped microparticles formed by selective adsorption of colloids. *J. Am. Chem. Soc.* **2011**, *133*, 5516–5524.
- (8) Sacanna, S.; Irvine, W. T. M.; Chaikin, P. M.; Pine, D. J. Lock and key colloids. *Nature* **2010**, *464*, 575–578.
- (9) Kim, J.-W.; Larsen, R. J.; Weitz, D. A. Synthesis of nonspherical colloidal particles with anisotropic properties. *J. Am. Chem. Soc.* **2006**, *128*, 14374–14377.
- (10) Park, J.-G.; Forster, J. D.; Dufresne, E. R. High-yield synthesis of monodisperse dumbbell-shaped polymer nanoparticles. *J. Am. Chem. Soc.* **2010**, *132*, 5960–5961.
- (11) Champion, J. A.; Katre, Y. K.; Mitragotri, S. Making polymeric micro- and nanoparticles of complex shapes. *Proc. Natl. Acad. Sci. U.S.A.* **2007**, *104*, 11901–11904.
- (12) Kim, S.-H.; Cho, Y.-S.; Jeon, S.-J.; Eun, T. H.; Yi, G.-R.; Yang, S.-M. Microspheres with tunable refractive index by controlled assembly of nanoparticles. *Adv. Mater.* **2008**, *20*, 3268–3273.
- (13) Xu, Q.; Hashimoto, M.; Dang, T. T.; Hoare, T.; Kohane, D. S.; Whitesides, G. M.; Langer, R.; Anderson, D. G. Preparation of monodisperse biodegradable polymer microparticles using a microfluidic flow-focusing device for controlled drug delivery. *Small* **2009**, *5*, 1575–1581.
- (14) Okubo, M.; Saito, N.; Fujibayashi, T. Preparation of polystyrene/poly(methyl methacrylate) composite particles having a dent. *Colloid Polym. Sci.* **2005**, *283*, 691–698.
- (15) Saito, N.; Kagari, Y.; Okubo, M. Effect of colloidal stabilizer on the shape of polystyrene/poly(methyl methacrylate) composite particles prepared in aqueous medium by the solvent evaporation method. *Langmuir* **2006**, *22*, 9397–9402.
- (16) Jeon, S.-J.; Yi, G.-R.; Yang, S.-M. Cooperative assembly of block copolymers with deformable interfaces: Toward nanostructured particles. *Adv. Mater.* **2008**, *20*, 4103–4108.
- (17) Kim, J. H.; Jeon, T. Y.; Choi, T. M.; Shim, T. S.; Kim, S.-H.; Yang, S.-M. Droplet microfluidics for producing functional microparticles. *Langmuir* **2014**, *30*, 1473–1488.
- (18) Jeong, J.; Um, E.; Park, J.-K.; Kim, M. W. One-step preparation of magnetic Janus particles using controlled phase separation of polymer blends and nanoparticles. *RSC Adv.* **2013**, *3*, 11801–11806.
- (19) Kumar, A.; Park, B. J.; Tu, F.; Lee, D. Amphiphilic Janus particles at fluid interfaces. *Soft Matter* **2013**, *9*, 6604–6617.
- (20) Kim, S.-H.; Kim, J. W.; Kim, D.-H.; Han, S.-H.; Weitz, D. A. Enhanced-throughput production of polymersomes using a parallelized capillary microfluidic device. *Microfluid. Nanofluid.* **2013**, *14*, 509–514.
- (21) Bae, W. K.; Kwak, J.; Park, J. W.; Char, K.; Lee, C.; Lee, S. Highly efficient green-light-emitting diodes based on CdSe@ZnS quantum dots with a chemical-composition gradient. *Adv. Mater.* **2009**, *21*, 1690–1694.
- (22) Utada, A. S.; Fernandez-Nieves, A.; Stone, H. A.; Weitz, D. A. Dripping to jetting transitions in coflowing liquid streams. *Phys. Rev. Lett.* **2007**, *99*, 094502.
- (23) Torza, S.; Mason, S. G. Three-phase interactions in shear and electrical fields. *J. Colloid Interface Sci.* **1970**, *33*, 67–83.
- (24) Brandrup, J.; Immergut, E. H.; Grulke, E. A. Polymer-Solvent Interaction Parameters. *Polymer Handbook*, 3; Wiley-Interscience: New York, 2003; pp VII/247–264.
- (25) Yang, P.; Wang, S.; Teng, X.; Wei, W.; Dravid, V. P.; Huang, L. Effect of magnetic nanoparticles on the morphology of polystyrene-b-poly(methyl methacrylate) diblock copolymer thin film. *J. Phys. Chem. C* **2012**, *116*, 23036–23040.
- (26) Brakke, K. A. The surface evolver. *Exp. Math.* **1992**, *1*, 141–165.
- (27) Datta, S. S.; Kim, S.-H.; Paulose, J.; Abbaspourrad, A.; Nelson, D. R.; Weitz, D. A. Delayed buckling and guided folding of inhomogeneous capsules. *Phys. Rev. Lett.* **2012**, *109*, 134302.
- (28) Choi, C.-H.; Weitz, D. A.; Lee, C.-S. One step formation of controllable complex emulsions: From functional particles to simultaneous encapsulation of hydrophilic and hydrophobic agents into desired position. *Adv. Mater.* **2013**, *25*, 2536–2541.
- (29) Marquis, M.; Renard, D.; Cathala, B. Microfluidic generation and selective degradation of biopolymer-based Janus microbeads. *Biomacromolecules* **2012**, *13*, 1197–1203.
- (30) Hwang, D. K.; Oakey, J.; Toner, M.; Arther, J. A.; Anseth, K. S.; Lee, S.; Zeiger, A.; Van Vliet, K. J.; Doyle, P. S. Stop-flow lithography for the production of shape-evolving degradable microgel particles. *J. Am. Chem. Soc.* **2009**, *131*, 4499–4504.